Available online at www.sciencedirect.com
SCIENCE DIRECT®
PERGAMON
International Journal of Non-Linear Mechanics 39 (2004) 795–809
INTERNATIONAL JOURNAL OF NON-LINEAR MECHANICS
www.elsevier.com/locate/nlm

# The effect of the slip condition on Stokes and Couette flows due to an oscillating wall: exact solutions

A.-R.A. Khaled[a], K. Vafai[b,*]

[a] *Department of Mechanical Engineering, The Ohio State University, Columbus, OH 43210, USA*
[b] *Department of Mechanical Engineering, University of California, Riverside, A 363 Bourns Hall, Riverside, CA 92521 0425, USA*

**Abstract**

Stokes and Couette flows produced by an oscillatory motion of a wall are analyzed under conditions where the no-slip assumption between the wall and the fluid is no longer valid. The motion of the wall is assumed to have a generic sinusoidal behavior. The exact solutions include both steady periodic and transient velocity profiles. It is found that slip conditions between the wall and the fluid produces lower amplitudes of oscillations in the flow near the oscillating wall than when no-slip assumption is utilized. Further, the relative velocity between the fluid layer at the wall and the speed of the wall is found to overshoot at a specific oscillating slip parameter or vibrational Reynolds number at certain times. In addition, it is found that wall slip reduces the transient velocity for Stokes flow while minimum transient effects for Couette flow is achieved only for large and small values of the wall slip coefficient and the gap thickness, respectively. The time needed to reach to steady periodic Stokes flow due to sine oscillations is greater than that for cosine oscillations with both wall slip and no-slip conditions.


*Keywords:* Stokes flow; Couette flow; Oscillations; Steady periodic velocity; Transient velocity; Wall slip

## 1. Introduction

The flow of viscous fluid induced by an oscillating shearing motion of a wall is found in many engineering applications such as flows in vibrating media. This problem is termed as Stokes second problem by Schilchting [1] if the fluid is bounded only by the moving wall. However, it is termed as Couette flow if the fluid is bounded by two parallel walls. The solution to the Stokes problem under vibrating wall conditions that satisfies non-slip conditions at the wall has been studied in depth by Erdogan [2]. He indicated that the study of Stokes flow due to a vibrating wall are found many in many applied problems such as in acoustic streaming around an oscillating body. The unsteady Couette flow problem has been considered in several works containing various effects as in the work of Jha [3] who introduced both magnetic and natural convection effects on the Couette flow between two vertical plates. The effects of fluid slippage at the wall for Couette flow are considered in the work of Marques et al. [4] under steady state conditions and only for gases. However, the literature

* Corresponding author. Tel.: +1-909-787-2135; fax: +1-909-787-2899.
*E-mail address:* vafai@engr.ucr.edu (K. Vafai).

0020-7462/04/$ - see front matter © 2003 Elsevier Ltd. All rights reserved.
doi:10.1016/S0020-7462(03)00043-X

**Nomenclature**

| | |
|---|---|
| $h$ | distance between the plates |
| $U, u$ | dimensionless and dimensional velocities |
| $\bar{U}, \bar{u}$ | dimensionless and dimensional velocity in $s$-domain |
| $u_o$ | reference velocity |
| $u_w$ | velocity of the vibrated plate |
| $R$ | vibrational Reynolds number |
| $R_o$ | dimensionless amplitude of the wall velocity |
| $t$ | time |
| $Y, y$ | dimensionless and dimensional normal coordinates |

*Greek symbols*

| | |
|---|---|
| $\beta$ | wall slip coefficient |
| $\lambda$ | oscillating slip parameter |
| $\upsilon$ | kinematic viscosity |
| $\tau$ | dimensionless time |
| $\omega$ | Frequency of the vibration |

lacks studies that take into account the possibility of fluid slippage at the walls under vibrating conditions. This problem appears in some applications such as in microchannels or nanochannels and in applications where a thin film of light oil is attached to the moving plates or when the surface is coated with special coatings such as a thick monolayer of hydrophobic octadecyltrichlorosilane [5]. Also, wall slip can occur if the working fluid contains concentrated suspensions [6].

When the molecular mean free path length of the fluid is comparable to the distance between the plates as in nanochannels or microchannels for Couette flows, the fluid exhibits non-continuum effects such as slip-flow as demonstrated experimentally by Derek et al. [5]. Navier [7] proposed boundary conditions that consider the possibility of fluid slip at a solid boundary nearly before two hundred years. This condition states that the velocity of the fluid at the plate is linearly proportional to the shear stress at the plate. Also, one could impose non-linear slip boundary conditions (e.g. [8]). To the author's knowledge the closed-form expressions for steady periodic and transient velocity field have not been given before under slip conditions for either Stokes or Couette flows. The developed solutions are important since their results can determine whether wall slip produces favorable effects such as reductions in the time required for attaining steady periodic flows or whether they need to be eliminated.

The velocity field for the Stokes and Couette flow can serve as a good estimate for the starting velocity for more complex flows such as gas flows induced by both natural convection (see Ref. [9]) and vibrations with wall slip conditions. This will reduce the computational time needed to reach steady periodic velocity and temperature for these complex flows. In this work, exact solutions for both Stokes and Couette flows subject to slip conditions are presented for both small and large times. The inverse transform for the solution of the Laplace transformed equation is solved using the theory of Residues and complex analysis which is an important tool which is infrequently used in literature. It is worth noting that while the Navier–Stokes equations and boundary conditions are in general non-linear, we are considering a linear problem. This work will form a basis for future works taking into considerations non-linear aspects of wall slip in vibrating conditions.

## 2. The Stokes flow

### 2.1. Basic equations

Consider a plane wall that is initially at rest and then it is allowed to move along the wall direction. The fluid over that wall is initially at rest and fills the region $y \geqslant 0$ where $y = 0$ is at the wall. The $y$-axis is the coordinate normal to the wall. The governing equation is

$$\frac{\partial u}{\partial t} = \upsilon \frac{\partial^2 u}{\partial y^2}, \tag{1}$$

where $u(y,t)$, $t$ and $\upsilon$ are the velocity in the $x$-direction which is along the wall direction, time and the kinematic viscosity of the fluid, respectively. Here we consider the existence of slip between the velocity of the fluid at the wall $u(0,t)$ and the speed of the wall. The relative velocity between $u(0,t)$ and the wall is assumed to be proportional to the shear rate at the wall. Accordingly, the boundary and initial conditions are

$$u(0,t) - \beta \frac{\partial u(0,t)}{\partial y} = u_w,$$

$$u(y,0) = 0,$$

$$u(y \to \infty, t) = 0, \tag{2}$$

where $\beta$ is the slip coefficient. The speed of the wall, $u_w$, for Stokes problem is taken to have either cosine or sine forms according to the following relations:

$$u_w = u_o \cos(\omega t), \tag{3a}$$

$$u_w = u_o \sin(\omega t), \tag{3b}$$

where $\omega$ is the frequency of the vibration. The Laplace transform method is used to solve Eq. (1). The Laplace transform of $u$ is defined by

$$\bar{u} = \int_0^\infty u e^{-st}\, dt. \tag{4}$$

Eq. (1) is transformed to

$$\bar{u}'' - \frac{s}{\upsilon}\bar{u} = 0, \tag{5}$$

where the prime indicates differentiation with respect to $y$. Transforming the boundary conditions where the oscillations have a cosine form result in

$$\bar{u}(0,s) - \beta \bar{u}'(0,s) = u_o \frac{s}{s^2 + \omega^2}, \Big/ \bar{u}(y \to \infty, s) = 0. \tag{6}$$

The boundary condition at the wall changes to the following for wall speed having a sine form:

$$\bar{u}(0,s) - \beta \bar{u}'(0,s) = u_o \frac{\omega}{s^2 + \omega^2}. \tag{7}$$

The solutions to Eq. (5) subject to boundary conditions (6) and (7) are given in Eqs. (8) and (9), respectively.

$$\frac{\bar{u}(y,s)}{u_o} = \frac{s e^{-\sqrt{\frac{s}{\upsilon}}y}}{\left(1 + \beta\sqrt{\frac{s}{\upsilon}}\right)(s^2 + \omega^2)}, \tag{8}$$

$$\frac{\bar{u}(y,s)}{u_o} = \frac{\omega e^{-\sqrt{\frac{s}{\upsilon}}\,y}}{\left(1+\beta\sqrt{\frac{s}{\upsilon}}\right)(s^2+\omega^2)}. \tag{9}$$

## 2.2. Exact solutions

### 2.2.1. Solution for cosine oscillations at the wall for positive values of $\beta$

Eqs. (8) and (9) have simple poles at $s=-i\omega$ and $s=i\omega$ and one branch point at $s=0$. It has another simple pole located at $s=\upsilon/\beta^2$ for negative values of $\beta$. However, the solution corresponding to this pole will be discussed later on. The characteristics of the inverse transform integral is that it vanishes in the left plane of the complex domain for large values of s and as s goes to zero. Therefore this integral can be shown by the Cauchy's residue theorem [10] to be equal to the sum of the residuals at $s=-i\omega$ and $s=i\omega$ and the inverse transform integral along $e^{i\pi}$ and $e^{-i\pi}$ directions. The solution to Eq. (8) for positive values of $\beta$ is found to be

$$\frac{u(\eta,\tau)}{u_o} = \frac{u_{sp}}{u_o} - \frac{1}{\pi}\int_0^\infty \frac{re^{-r\tau}}{(r^2+1)}\left[\frac{\sin(\sqrt{r}\eta)+\lambda\sqrt{2r}\cos(\sqrt{r}\eta)}{1+2\lambda^2 r}\right] dr, \tag{10}$$

where $\eta$, $\tau$ and $\lambda$ are the transformed normal coordinate, dimensionless time and the oscillatory slip parameter which are given as

$$\eta = y\sqrt{\frac{\omega}{\upsilon}}, \quad \tau=\omega t, \quad \lambda=\beta\sqrt{\frac{\omega}{2\upsilon}}. \tag{11}$$

The steady periodic velocity of the fluid is

$$\frac{u_{sp}(\eta,\tau)}{u_o} = \left[\frac{(1+\lambda)\cos\left(\tau-\frac{\eta}{\sqrt{2}}\right)+\lambda\sin\left(\tau-\frac{\eta}{\sqrt{2}}\right)}{2\lambda^2+2\lambda+1}\right] e^{-\eta/\sqrt{2}}. \tag{12}$$

Note that last term in Eq. (10) vanishes for large times and therefore it represents the transient aspect of the fluid velocity. The steady periodic relative velocity between the velocity of the fluid at the wall and the wall itself can be found

$$\frac{u_{rel}(\tau)}{u_o} \equiv \frac{u_{sp}(0,\tau)}{u_o} - \cos(\tau) = \frac{\lambda(\sin(\tau)-\cos(\tau))-2\lambda^2\cos(\tau)}{2\lambda^2+2\lambda+1}. \tag{13}$$

The transient velocity which is obtained by subtracting Eq. (12) from Eq. (10) has the flowing form:

$$\frac{u_t(\eta,\tau)}{u_o} = -\frac{1}{\pi}\int_0^\infty \frac{re^{-r\tau}}{(r^2+1)}\left[\frac{\sin(\sqrt{r}\eta)+\lambda\sqrt{2r}\cos(\sqrt{r}\eta)}{1+2\lambda^2 r}\right] dr. \tag{14}$$

For large times, this velocity approaches zero asymptotically along the following asymptote for lower values of both the dimensionless coordinate $\eta$ and the oscillating slip parameter:

$$\frac{u_t(\eta,\tau)}{u_o} \approx -\frac{3}{4\sqrt{\pi}}\frac{(\eta+\sqrt{2}\lambda)}{\tau^{5/2}} \quad \text{as } \tau\to\infty. \tag{15}$$

The plot of the steady periodic velocity of the fluid is shown in Fig. 1. The dotted line represents a case where slip between the wall and the fluid is present. The oscillations in fluid velocities are noticed to decrease as this slip is increased. The slip increases as the oscillating slip parameter $\lambda$ increases as shown in Fig. 2.

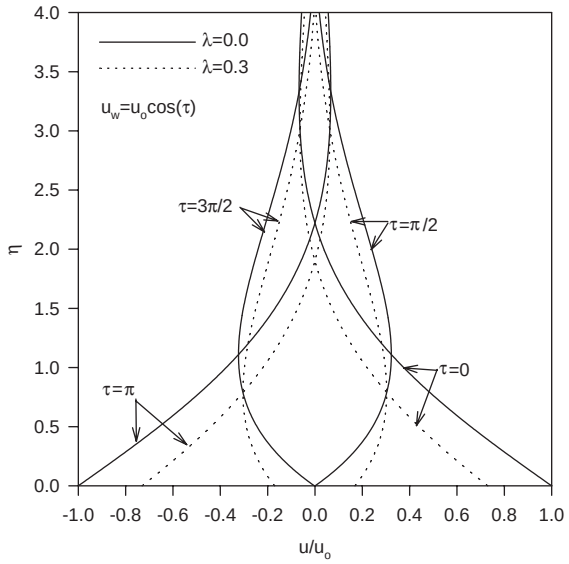


Fig. 1. Effects of the oscillating slip parameter on the steady periodic velocity profile (Stokes flow).

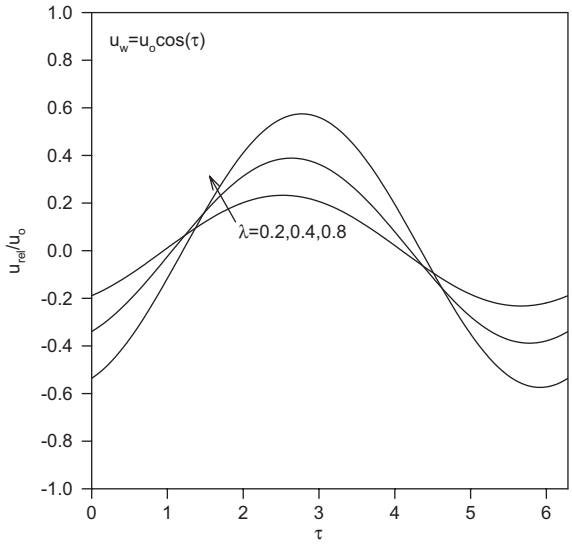


Fig. 2. Effects of the oscillating slip parameter on the steady wall slip velocity (Stokes flow).

*2.2.2. Solution for the sine oscillations of the boundary for positive values of β*

The solution to Eq. (9) can be obtained by a similar method discussed earlier. Accordingly, the velocity of the fluid for positive values of $\beta$ is found to be

$$\frac{u(\eta,\tau)}{u_o} = \frac{u_{sp}}{u_o} + \frac{1}{\pi}\int_0^\infty \frac{e^{-r\tau}}{(r^2+1)}\left[\frac{\sin(\sqrt{r}\eta)+\lambda\sqrt{2r}\cos(\sqrt{r}\eta)}{1+2\lambda^2 r}\right] dr. \tag{16}$$

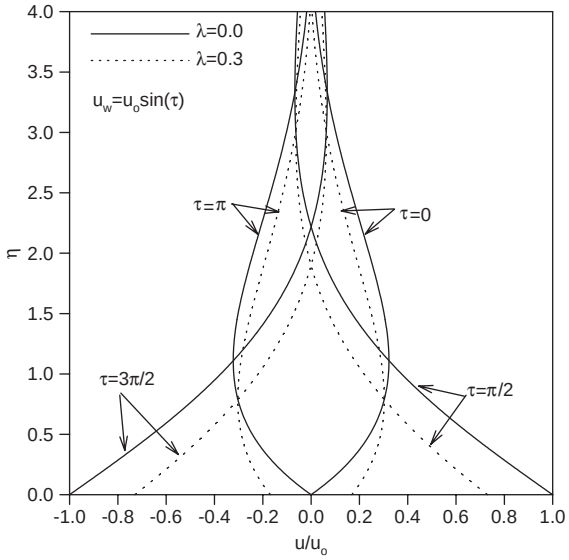


Fig. 3. Effects of the oscillating slip parameter on the steady periodic velocity profile (Stokes flow).

The steady periodic velocity of the fluid is

$$\frac{u_{\mathrm{sp}}(\eta,t)}{u_{\mathrm{o}}}=\left[\frac{(1+\lambda)\sin\left(\tau-\dfrac{\eta}{\sqrt{2}}\right)-\lambda\cos\left(\tau-\dfrac{\eta}{\sqrt{2}}\right)}{2\lambda^2+2\lambda+1}\right]\mathrm{e}^{-\eta/\sqrt{2}}, \tag{17}$$

where $\eta$, $\tau$ and $\lambda$ are similar to those defined in the last case. The steady periodic relative velocity between the velocity of the fluid at the wall and the wall speed is calculated from the following:

$$\frac{u_{\mathrm{rel}}(\tau)}{u_{\mathrm{o}}}\equiv\frac{u_{\mathrm{sp}}(0,\tau)}{u_{\mathrm{o}}}-\sin(\tau)=-\frac{\lambda(\sin(\tau)+\cos(\tau))+2\lambda^2\sin(\tau)}{2\lambda^2+2\lambda+1}. \tag{18}$$

The transient velocity which is obtained by subtracting Eq. (17) from Eq. (16) has the following form:

$$\frac{u_{\mathrm{t}}(\eta,\tau)}{u_{\mathrm{o}}}=\frac{1}{\pi}\int_0^\infty\frac{\mathrm{e}^{-r\tau}}{(r^2+1)}\left[\frac{\sin(\sqrt{r}\eta)+\lambda\sqrt{2r}\cos(\sqrt{r}\eta)}{1+2\lambda^2 r}\right]\mathrm{d}r. \tag{19}$$

The transient velocity is also found to vanish for larger times. It can be shown that it approaches zero asymptotically along the following asymptote for lower values of both the dimensionless coordinate $\eta$ and the oscillating slip parameter:

$$\frac{u_{\mathrm{t}}(\eta,\tau)}{u_{\mathrm{o}}}\approx\frac{1}{2\sqrt{\pi}}\frac{(\eta+\sqrt{2}\lambda)}{\tau^{3/2}}\quad\text{as }\tau\to\infty. \tag{20}$$

Similar trends as the previous case with a phase shift are noticed for the steady periodic velocities and the slip velocity. These trends are shown in Figs. 3 and 4. A wall having a motion in cosine form is found to have less transient effects than when the motion is expressed in sine form. This is clearly seen from Eqs. (15) and (20). A dimensionless slip parameter of a value equal to $1/\sqrt{2}$ is found to cause a maximum slip speed between the wall and the fluid as shown in Fig. 5. This can be shown using Eq. (15). An interesting feature exhibited by slip effects is that they tend to increase the transient effects especially at the wall as predicted by

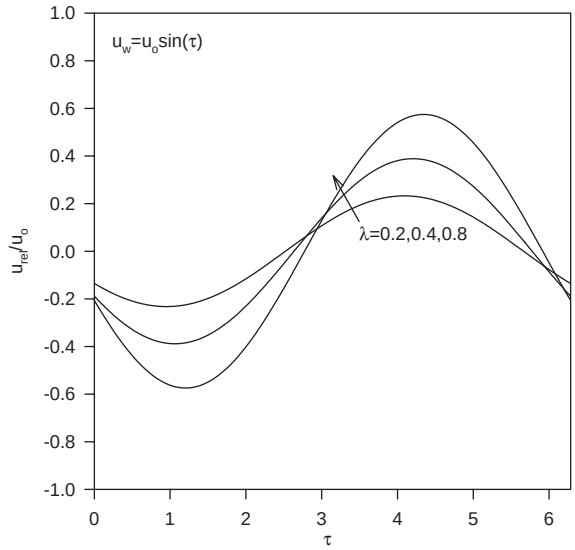


Fig. 4. Effects of the oscillating slip parameter on the steady wall slip velocity (Stokes flow).

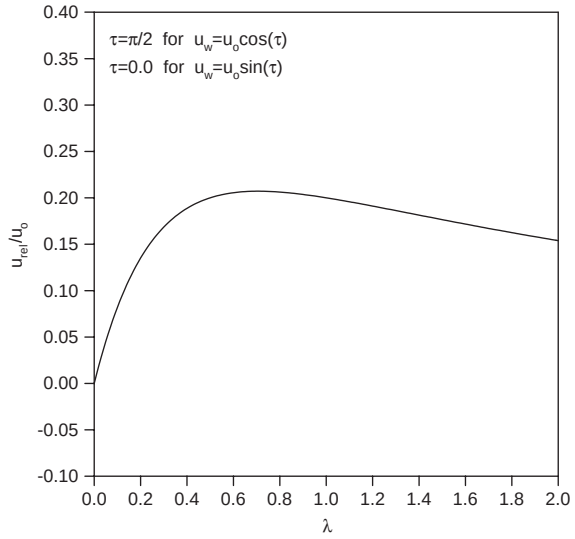


Fig. 5. Effects of large range of the oscillating slip parameter on the slip velocity at a specific time (Stokes flow).

Eqs. (15) and (20). It is worth noting that negative values of $\beta$ results in non-vanishing transient terms at large times indicating that cases with negative values of $\beta$ do not represent physical cases.

Fig. 6 illustrates the effects of the oscillating slip parameter on the transient velocity for both cosine, $u_w = -u_o \cos(\tau)$, and sine oscillations. This figure shows that flow due to cosine oscillations reach steady periodic values faster than for sine oscillations. Also, Fig. 6 shows that transient velocity increases near the wall as the oscillating slip parameter increases but the maximum transient velocity which occur far from the wall decreases as the oscillating slip parameter increases. Over all, it is found that an increase in the oscillating slip parameter causes a small reduction in the time needed to reach to the steady periodic flow.

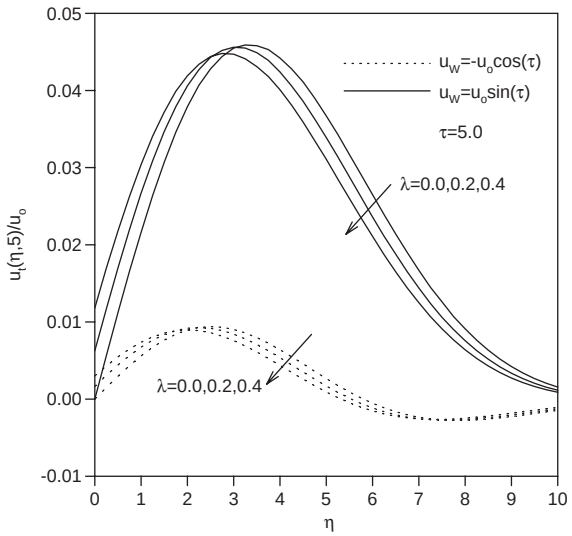


Fig. 6. Effects of the oscillating slip parameter on the transient velocity profile (Stokes flow).

For the values of the oscillating slip parameter listed in Fig. 6, the time needed to reach to steady periodic flow due to sine oscillations is found to be about $\tau \cong 21$ while it is about $\tau \cong 4.7$ for cosine oscillations, evaluated with $\Delta r = 0.01$. These values were obtained by computing the dimensionless times needed for the maximum dimensionless transient velocity to reach 0.01. The reported values are greater than those values reported by Erdogan [2] because the latter selected a different criterion for calculating these times. There is an agreement between the results of Fig. 6 at no slip conditions for the sine oscillations and the corresponding results that can be extracted from the first figure in the work of Erdogan [2].

## 3. The Couette flow

### 3.1. Basic equations

Consider a thin film that is initially at rest and then one of its plates is allowed to oscillate in the direction of its length. The fluid inside the thin film is also initially at rest. The fluid exists in the region $0 \leqslant y \leqslant h$ where the $y$-axis is the coordinate normal to the flow and $h$ is the thickness of the thin film. The vibrated wall is located at $y = 0$ while the fixed wall is at $y = h$. The flow inside the thin film is induced by vibrations that are assumed to be present at $y = 0$ and to be along the flow direction. The velocity of the lower plate, $u_w$, is chosen to be similar to Eq. (3b). The governing equation is Eq. (1). The boundary conditions due to wall slip as well as the initial condition are

$$u(0,t) - \beta \frac{\partial u(0,t)}{\partial y} = u_o \sin(\omega t),$$

$$u(h,t) + \beta \frac{\partial u(h,t)}{\partial y} = 0,$$

$$u(y,0) = 0. \tag{21}$$

The previous equation can be normalized using the following dimensionless parameters:

$$\tau = \omega t, \quad U = \frac{u}{h\omega}, \quad Y = \frac{y}{h}. \tag{22}$$

Accordingly, Eq. (1) reduces to

$$\frac{\partial U}{\partial \tau} = \frac{1}{R}\frac{\partial^2 U}{\partial Y^2} \tag{23}$$

and the boundary conditions reduce to

$$\begin{aligned} &U(0,\tau) - \frac{\beta}{h}\frac{\partial U(0,\tau)}{\partial Y} = R_o \sin(\tau), \\ &U(1,\tau) + \frac{\beta}{h}\frac{\partial U(1,\tau)}{\partial Y} = 0, \\ &U(Y,0) = 0, \end{aligned} \tag{24}$$

where $R$ and $R_o$ are defined as follows:

$$R = \frac{h^2\omega}{\upsilon}, \quad R_o = \frac{u_o}{h\omega} \tag{25}$$

$R$ is named the vibrational Reynolds number and $R_o$ represents the ratio between the lateral Reynolds number to the vibrational Reynolds number. The solution of the Laplace transform of Eq. (23) is

$$\begin{aligned} \frac{\bar{U}(Y,s)}{R_o} = &- \frac{\left[\cosh(\sqrt{Rs}) + \left(\frac{\beta}{h}\right)\sqrt{Rs}\sinh(\sqrt{Rs})\right]\sinh(\sqrt{Rs}Y)}{(s^2+1)\left[\left(1+\left(\frac{\beta}{h}\right)^2 Rs\right)\sinh(\sqrt{Rs}) + 2\left(\frac{\beta}{h}\right)\sqrt{Rs}\cosh(\sqrt{Rs})\right]} \\ &+ \frac{\left[\sinh(\sqrt{Rs}) + \left(\frac{\beta}{h}\right)\sqrt{Rs}\cosh(\sqrt{Rs})\right]\cosh(\sqrt{Rs}Y)}{(s^2+1)\left[\left(1+\left(\frac{\beta}{h}\right)^2 Rs\right)\sinh(\sqrt{Rs}) + 2\left(\frac{\beta}{h}\right)\sqrt{Rs}\cosh(\sqrt{Rs})\right]}. \end{aligned} \tag{26}$$

### 3.2. Exact solution

Eq. (26) has simple poles at $s = -\mathrm{i}$ and $s = i$. Also, this equation has an infinite number of poles located on the negative real axis at $s = -j_n^2/R$ where $j_n$ is a real number and $n$ is the index integer number of the pole changing from one to infinity where $j_n$ can be found by the following equation:

$$\tan(j_n) = -\frac{2\frac{\beta}{h}j_n}{1-\left(\frac{\beta}{h}\right)^2 j_n^2}. \tag{27}$$

The poles that are located at $s = -j_n^2/R$ are responsible for the transient behavior of the velocity. The Laplace inverse for $\bar{U}$ can be calculated from the following relation:

$$\frac{U(Y,\tau)}{R_o} = \sum_{n=1}^{\infty} \mathrm{Res}[\bar{U}(Y,s)\mathrm{e}^{s\tau}]_{-\frac{j_n^2}{R}} + \mathrm{Res}[\bar{U}(Y,s)\mathrm{e}^{s\tau}]_{-\mathrm{i}} + \mathrm{Res}[\bar{U}(Y,s)\mathrm{e}^{s\tau}]_{\mathrm{i}}, \tag{28}$$

where Res designate the residue. Evaluating the residues at all $s = -j_n^2/R$ results in the transient velocity profile. It is

$$U_t(Y,\tau) = \frac{R_o}{R}\sum_{n=1}^{\infty}\frac{F_1(j_n,Y)}{F_2(j_n)}\,e^{-j_n^2\tau/R}, \tag{29a}$$

where $F_1$ and $F_2$ are calculated from the following equations:

$$F_1(j_n,Y) = \left(\sin(j_n) + \left(\frac{\beta}{h}\right) j_n\cos(j_n)\right)\cos(j_nY) - \left(\cos(j_n) - \left(\frac{\beta}{h}\right) j_n\sin(j_n)\right)\sin(j_nY), \tag{29b}$$

$$F_2(j_n) = \left(\frac{j_n^4}{R^2}+1\right)\left[\left(\frac{\beta}{h}\right)\left(\frac{\beta}{h}+1\right)\sin(j_n) - \left(1+2\left(\frac{\beta}{h}\right) - j_n^2\left(\frac{\beta}{h}\right)^2\right)\frac{\cos(j_n)}{2j_n}\right].$$

It is noticed that the transient solution described in Eq. (29) vanishes for large times as long as $\beta$ is positive. If $\beta$ is negative, then Eq. (26) may have another pole located on the positive real axis which does not lead to a physical case as in the analysis of the Stokes flow. The steady periodic velocity is obtained by evaluating the residues at $s = -\mathrm{i}$ and $s = \mathrm{i}$ and it is equal to

$$\begin{aligned}\frac{U_{sp}(Y,\tau)}{R_o} = &-\frac{(M_1M_3+M_2M_4)(f_1(Y)\sin(\tau)+f_2(Y)\cos(\tau))}{M_3^2+M_4^2}\\ &-\frac{(M_1M_4-M_2M_3)(f_2(Y)\sin(\tau)-f_1(Y)\cos(\tau))}{M_3^2+M_4^2}\\ &+\frac{(M_3M_5+M_4M_6)(f_3(Y)\sin(\tau)+f_4(Y)\cos(\tau))}{M_3^2+M_4^2}\\ &+\frac{(M_3M_6-M_4M_5)(f_3(Y)\cos(\tau)-f_4(Y)\sin(\tau))}{M_3^2+M_4^2},\end{aligned} \tag{30a}$$

where the functions $f_1$, $f_2$, $f_3$ and $f_4$ are defined as follows

$$f_1(Y) = \sinh\left(\sqrt{\frac{R}{2}}Y\right)\cos\left(\sqrt{\frac{R}{2}}Y\right), \quad f_2(Y) = \cosh\left(\sqrt{\frac{R}{2}}Y\right)\sin\left(\sqrt{\frac{R}{2}}Y\right)$$

$$f_3(Y) = \cosh\left(\sqrt{\frac{R}{2}}Y\right)\cos\left(\sqrt{\frac{R}{2}}Y\right), \quad f_4(Y) = \sinh\left(\sqrt{\frac{R}{2}}Y\right)\sin\left(\sqrt{\frac{R}{2}}Y\right) \tag{30b}$$

The constants $M_1$, $M_2$, $M_3$ and $M_4$ are calculated from the following:

$$M_1 = \cosh\left(\sqrt{\frac{R}{2}}\right)\cos\left(\sqrt{\frac{R}{2}}\right) + \alpha\sinh\left(\sqrt{\frac{R}{2}}\right)\cos\left(\sqrt{\frac{R}{2}}\right) - \alpha\cosh\left(\sqrt{\frac{R}{2}}\right)\sin\left(\sqrt{\frac{R}{2}}\right), \tag{30c}$$

$$M_2 = \sinh\left(\sqrt{\frac{R}{2}}\right)\sin\left(\sqrt{\frac{R}{2}}\right) + \alpha\cosh\left(\sqrt{\frac{R}{2}}\right)\sin\left(\sqrt{\frac{R}{2}}\right) + \alpha\sinh\left(\sqrt{\frac{R}{2}}\right)\cos\left(\sqrt{\frac{R}{2}}\right),$$

$$M_3 = \sinh\left(\sqrt{\frac{R}{2}}\right)\cos\left(\sqrt{\frac{R}{2}}\right) + 2\alpha\cosh\left(\sqrt{\frac{R}{2}}\right)\cos\left(\sqrt{\frac{R}{2}}\right) - 2\alpha^2\cosh\left(\sqrt{\frac{R}{2}}\right)\sin\left(\sqrt{\frac{R}{2}}\right) - 2\alpha\sinh\left(\sqrt{\frac{R}{2}}\right)\sin\left(\sqrt{\frac{R}{2}}\right),$$

$$M_4 = \cosh\left(\sqrt{\frac{R}{2}}\right)\sin\left(\sqrt{\frac{R}{2}}\right) + 2\alpha^2\sinh\left(\sqrt{\frac{R}{2}}\right)\cos\left(\sqrt{\frac{R}{2}}\right) + 2\alpha\sinh\left(\sqrt{\frac{R}{2}}\right)\sin\left(\sqrt{\frac{R}{2}}\right) + 2\alpha\cosh\left(\sqrt{\frac{R}{2}}\right)\cos\left(\sqrt{\frac{R}{2}}\right),$$

$$M_5 = \sinh\left(\sqrt{\frac{R}{2}}\right)\cos\left(\sqrt{\frac{R}{2}}\right) + \alpha\cosh\left(\sqrt{\frac{R}{2}}\right)\cos\left(\sqrt{\frac{R}{2}}\right) - \alpha\sinh\left(\sqrt{\frac{R}{2}}\right)\sin\left(\sqrt{\frac{R}{2}}\right),$$

$$M_6 = \cosh\left(\sqrt{\frac{R}{2}}\right)\sin\left(\sqrt{\frac{R}{2}}\right) + \alpha\sinh\left(\sqrt{\frac{R}{2}}\right)\sin\left(\sqrt{\frac{R}{2}}\right) + \alpha\cosh\left(\sqrt{\frac{R}{2}}\right)\cos\left(\sqrt{\frac{R}{2}}\right).$$

The parameter $\alpha$ is equal to

$$\alpha = \left(\frac{\beta}{h}\right)\sqrt{\frac{R}{2}}. \tag{30d}$$

Accordingly, the velocity field is the sum of the transient and steady periodic values:

$$U = U_t + U_{sp}. \tag{31}$$

### 3.3. Discussion

Fig. 7 shows the effect of the slip coefficient $\beta$ on the steady periodic velocity profile. As can be seen, fluctuations in flow velocities near the vibrated wall decrease as $\beta$ increases however they increase near the fixed wall. The effect of the vibrational Reynolds number $R$ on the absolute value of the fluids relative velocity at the vibrated plate is seen in Fig. 8 for two different times: $\tau=0$ and $\tau=\pi/2$. At these times the absolute wall speed is minimum and maximum, respectively. It is noticed that the absolute value of the relative velocity between the fluid layer adjacent to the vibrated plate and the speed of that plate is enhanced at certain values of $R$ at $\tau = 0$.

As seen from Fig. 8, the value of $R$ that maximizes the fluid-slip is found to decrease as $\beta$ increases. However, this phenomenon is not observed for $\tau = \pi/2$. The maximization at both studied times of the absolute value of the slip are also noticed for the behavior of the fluid layer adjacent to the fixed wall as a function of both the vibrational Reynolds number and the slip coefficient as depicted in Fig. 9. It is furthermore noticed from Fig. 9 that the no-slip condition at the fixed plate is recovered for large values of the vibrational Reynolds number. It is worth noting that the wall slip velocity at diminishing vibrational Reynolds number is the same near both plates and it is converging to following value $U(1,\tau) = (\beta/h)\sin(\tau)/[2(\beta/h) + 1]$.

Fig. 10 illustrates the effect of the slip coefficient $\beta$ on the steady periodic slip velocity at the vibrated plate. It is noticed that increasing the values of $\beta$ results in increases in the slip velocity at the vibrated plate at $\tau=\pi/2$. However at other times such as at $\tau=0$, the fluid slip decreases as $\beta$ increases for large vibrational Reynolds number as shown in Fig. 10. It should also be noted that the value of the slip coefficient that caused the maximum overshoot in fluid slip decreases as the vibrational Reynolds number increases at $\tau=0$. Fig. 11 illustrates the effect of the slip coefficient $\beta$ on the steady periodic slip velocity at the fixed plate. It is noticed

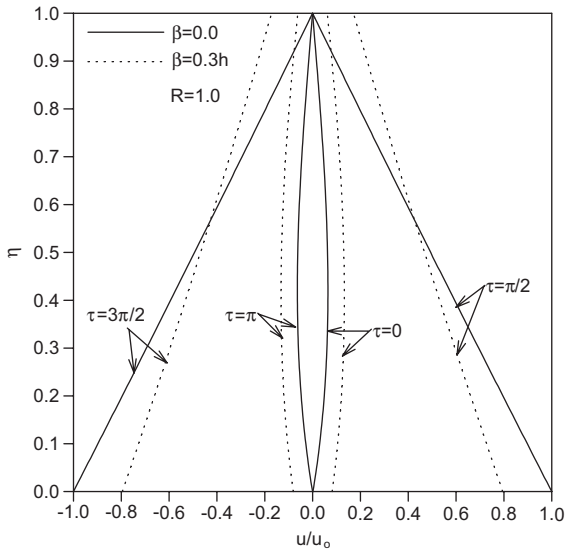


Fig. 7. Effects of the slip coefficient on the steady periodic velocity profile (Couette flow).

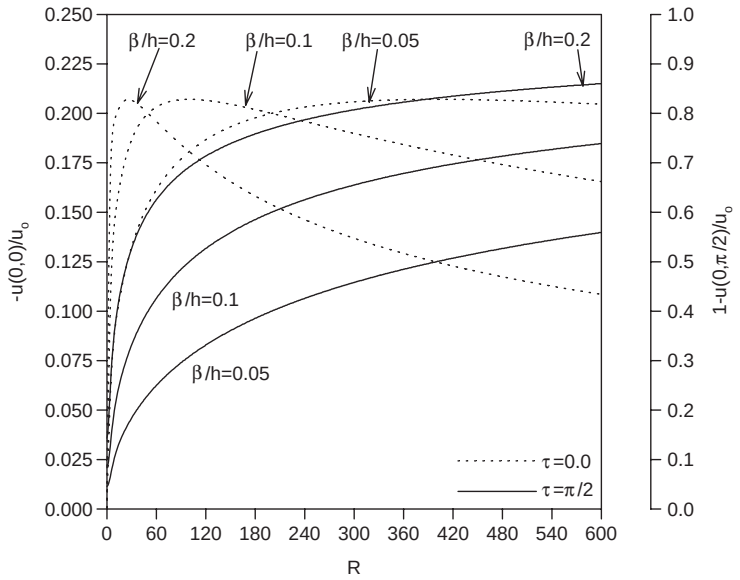


Fig. 8. Effects of the vibrational Reynolds number on the steady periodic slip velocity at $Y = 0$ (Couette flow).

that the maximum overshoot in the fluid slip at the fixed plate is also present here and that the critical value of $\beta$ that causes a maximum overshoot in the slip decreases as $R$ increases at both times.

The effects of the vibrational Reynolds number and the wall slip are shown in Fig. 12. The absolute value for transient velocity increases as $R$ increases since the latter cause a reduction in the diffusion process. Also, it is noticed that transient effects with wall slip is greater than with no-slip conditions yet at large values of

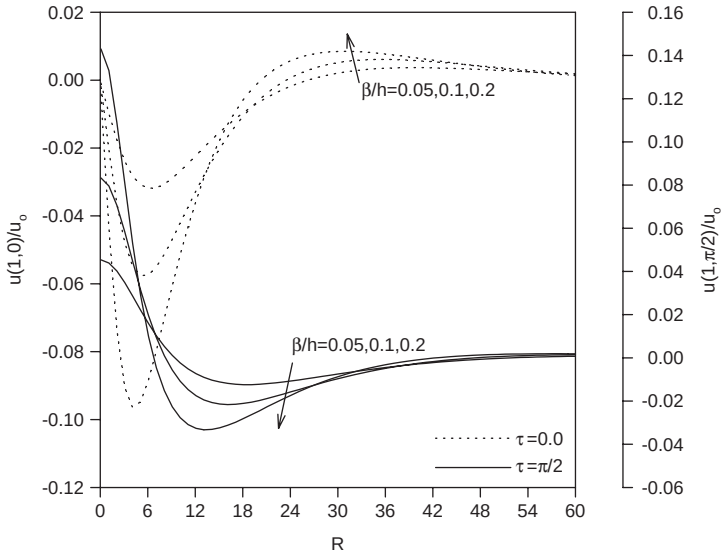


Fig. 9. Effects of the vibrational Reynolds number on the steady periodic slip velocity at $Y = 1$ (Couette flow).

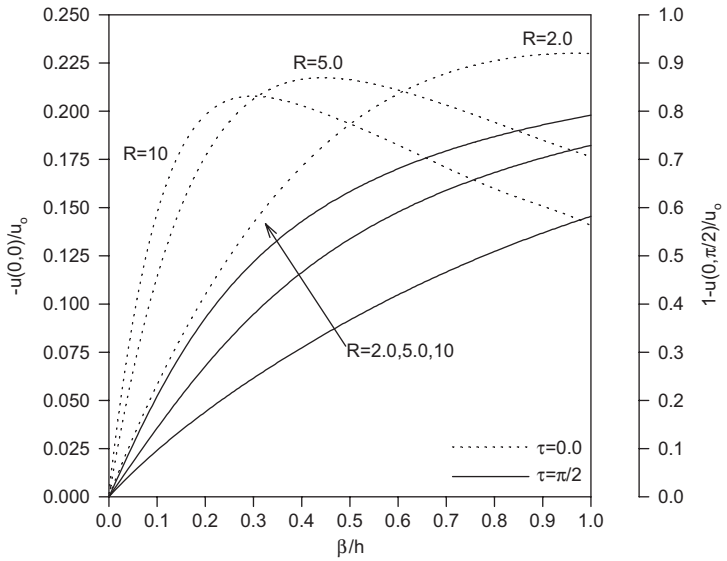


Fig. 10. Effects of the slip coefficient on the steady periodic slip velocity at $Y = 0$ (Couette flow).

$\beta/h$, the absolute value of the transient velocity decreases as wall slip coefficient increases as can be seen from Eq. (29). For intermediate values of $\beta/h$, the effect of wall slip on the transient velocity becomes more complex because the eigenfunctions of the transient solution given by Eq. (29) become strongly dependent on $\beta/h$.

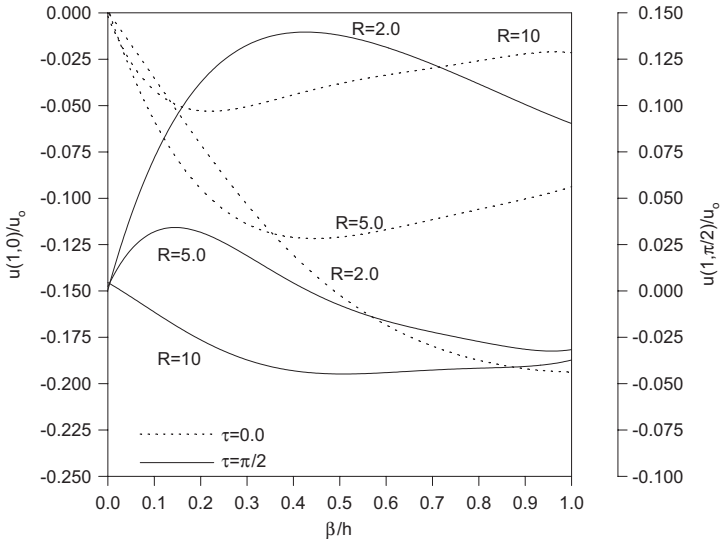


Fig. 11. Effects of the slip coefficient on the steady periodic slip velocity at $Y = 1$ (Couette flow).

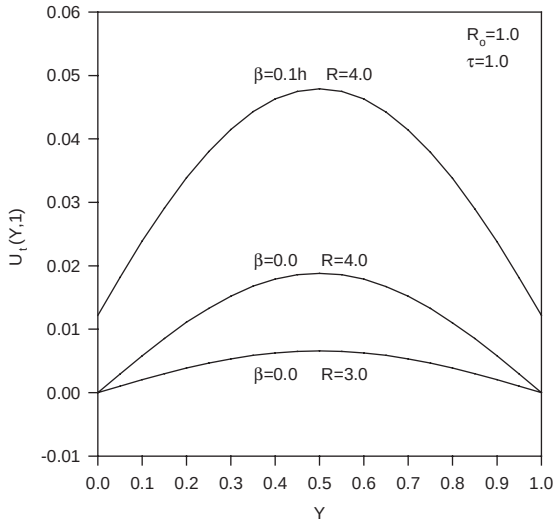


Fig. 12. Effects of the $\beta$ and $R$ on the transient velocity profile (Couette flow).

## 4. Conclusion

The effects of both the oscillation and the fluid-slip on the Stokes and Couette flows were studied. The velocity of the wall for Stokes flow was varied using sine and cosine forms while for the Couette flow, one wall was fixed and the other was subjected to oscillations. The governing equations were solved using the Laplace transformation domain. The Cauchy's residue theorem was used to obtain the inverse Laplace transform of the velocity. The transient part of the velocity was found to vanish for larger times for positive

values of the slip coefficient. It was found that fluid-slip reduced the oscillations in the fluid for both types of flows near the vibrating wall. For certain times, it was established that the fluid-slip at the oscillating plate is maximized for some values of the slip parameter and vibrational Reynolds number. However, in general the fluid-slip was found to increase with increases in the vibrational Reynolds number.

For the Couette flow case, the critical value of the slip coefficient that causes a maximum overshoot in the slip velocity at the vibrated wall was found to decrease with an increase in the vibrational Reynolds number at $\tau = 0$. The results for the Couette flow illustrated that the non-slip condition at the fixed plate is recovered at large vibrational Reynolds number. Further, it was found that wall slip reduces the transient velocity for Stokes flow while the minimum transient effects for the Couette flow is achieved only for large and small values of the wall slip coefficient and the gap thickness, respectively.

## Acknowledgements

We acknowledge partial support of this work by DOD/DARPA/DMEA under grant number DMEA90-02-2-0216.

## References

[1] H. Schilichting, Boundary Layer Theory, 6th Edition, McGraw-Hill, New York, 1968.
[2] M.E. Erdogan, A note on unsteady flow of a viscous fluid due to an oscillating plane wall, Int. J. Non-Linear Mech. 35 (2000) 1–6.
[3] B.K. Jha, Natural Convection in Unsteady MHD Couette Flow, Heat & Mass Transfer 37 (2001) 329–331.
[4] W. Marques Jr., G.M. Kremer, F.M. Sharipov, Couette flow with slip and jump boundary conditions, Continuum Mech. Thermodynam. 12 (2000) 379–386.
[5] C. Derek, D.C. Tretheway, C.D. Meinhart, Apparent fluid slip at hydrophobic microchannel walls, Phys. Fluids 14 (2002) L9–L12.
[6] F. Soltani, U. Yilmazer, Slip Velocity and Slip Layer Thickness in Flow of Concentrated Suspensions, J. Appl. Polym. Sci. 70 (1998) 515–522.
[7] C.L.M.H. Navier, Mem. Acad. Sci. Inst. France 1 (1823) 414–416.
[8] S. Yu, T.A. Ameel, Slip-flow Heat Transfer in Rectangular Microchannels, Int. J. Heat Mass Trans. 44 (2002) 4225–4234.
[9] M.P. Dyko, K. Vafai, A.K. Mojtabi, Numerical and Experimental Investigation of Stability of Natural Convective Flows Within a Horizontal Annulus, J. Fluid Mech. 381 (1999) 27–61.
[10] J.W. Brown, R.V. Churchill, Complex Variables and Applications, 6th Edition, McGraw-Hill, New York, 1996.